Applied Surface Science 478 (2019) 347–354

Contents lists available at ScienceDirect

Applied Surface Science

journal homepage: www.elsevier.com/locate/apsusc

Full Length Article

Highly selective ozone gas sensor based on nanocrystalline $Zn_{0.95}Co_{0.05}O$ thin film obtained via spray pyrolysis technique

Yina J. Onofre[a,*], Ariadne C. Catto[a], Sandrine Bernardini[c], Tomas Fiorido[c], Khalifa Aguir[c], Elson Longo[b], Valmor R. Mastelaro[d], Luís F. da Silva[a], Marcio P.F. de Godoy[a,*]

[a] Department of Physics, Universidade Federal de São Carlos - UFSCar, 13565-905 São Carlos, SP, Brazil
[b] Center for Development of Functional Materials, Universidade Federal de São Carlos - UFSCar, 13565-905 São Carlos, SP, Brazil
[c] Aix-Marseille University, CNRS IM2NP (UMR 7334), FS St Jérôme S152, Marseille, 13397, France
[d] Insitute of Physics of São Carlos, University of São Paulo, 13566-590 São Carlos, SP, Brazil

ARTICLE INFO

Keywords:
ZnCoO
Spray pyrolysis
Chemiresistor
Ozone, gas sensor, selectivity

ABSTRACT

Chemiresistors are highly important for monitoring and detection of harmful gases produced from industrial processes and vehicle emissions. We report herein an experimental investigation of the gas-sensing properties of $Zn_{0.95}Co_{0.05}O$ thin film deposited by spray pyrolysis technique. The X-ray photoelectron spectroscopy indicated the presence of Co^{2+} ions into de ZnO lattice. The gas-sensing measurements revealed the sensitivity of $Zn_{0.95}Co_{0.05}O$ film towards ozone gas in a wide range of concentrations from 20 to 1040 ppb, exhibiting good repeatability and total reversibility after consecutive exposures. Selectivity for ozone is observed in comparison to NO_2, NH_3, and CO gases even at low levels. This manuscript reports the effectiveness of spray-pyrolysis method for obtaining nanostructured $Zn_{1-x}Co_xO$ thin films for practical applications as an ozone gas sensor.

1. Introduction

The monitoring and environmental control of pollutants in the atmosphere has increased in the last two decades due to their harmful effects on human health and global warming [1–3]. Motor vehicles and industrial processes emissions are some of those responsible for the presence of primary and secondary pollutants in the lower atmosphere, such as O_3, CO, NO_x, NH_3, SO_2, etc. [4,5]. According to the values registered in the "2016 Annual Report" by CETESB - the Environmental Company of São Paulo State (Brazil), the ozone (O_3) levels were approximately 165 ppb (parts-per-billion) in São Paulo metropolitan region, above the value 100 ppb (8 h-mean daily of exposition) recommended by WHO (World Health Organization) [6]. Thereby the detection and the monitoring of O_3 gas, as well as other pollutants, require sensing materials exhibiting high sensitivity and stability, fast response and shorter recovery times [7].

The semiconducting metal oxides (SMO) have been considered a promising material class for gas sensors, presenting a high sensitivity towards several analytes (reducing and oxidizing), good stability, and also a low-cost of production facilitating thus the integration in sensor devices [8,9]. Traditionally, the SMO used as ozone gas-sensing are based on SnO_2 [10], In_2O_3 [11], ZnO [12,13] and WO_3 [14]. Particularly, ZnO is a II-VI semiconductor with a wide bandgap (3.37 eV at room temperature), commonly used in various applications as light emitting diodes (LED) [15], surface acoustic wave (SAW) devices [16] and transparent conductive oxides (TCO) [17] due to its electronic, optical and piezoelectric properties, as well as its low cost, abundance and non-toxicity. It has been satisfactorily applied as sensing material for detection of H_2 [18], NO_x [19], H_2S [20] and ethanol [21], emerging then as a promising material for sensor devices despite its low selectivity [22].

In the past decade, several approaches have been investigated in order to improve the gas sensing performance, mainly, by means of the enhancement of the surface-to-volume ratio with 1D nanostructures [12], noble metal addition (e.g., Au, Pt, Pd) [23], and doping with transition metals [24–26]. The doping process has been an effective approach to tune the electronic, microstructure, optical and magnetic properties of the material host, also improving its sensing performance [1,27–29]. In addition, the $Zn_{1-x}Co_xO$ solid solutions have been extensively studied in bandgap engineering [30] and also as diluted magnetic semiconductor (DMS) [31–33]. Recently, their application as sensing materials has shown an increase on sensor response and selectivity for gases such as NH_3 [34] liquefied petroleum gas (LPG) [35], H_2 [25] and ethanol [36] for concentrations above 100 ppm (parts-per-million). The Cobalt-doping introduces energy levels of impurities and defects, such as oxygen vacancies, that create active adsorption sites,

* Corresponding authors.
E-mail addresses: julieth@df.ufscar.br (Y.J. Onofre), mgodoy@ufscar.br (M.P.F. de Godoy).

https://doi.org/10.1016/j.apsusc.2019.01.197
Received 12 July 2018; Received in revised form 28 December 2018; Accepted 23 January 2019
Available online 24 January 2019
0169-4332/

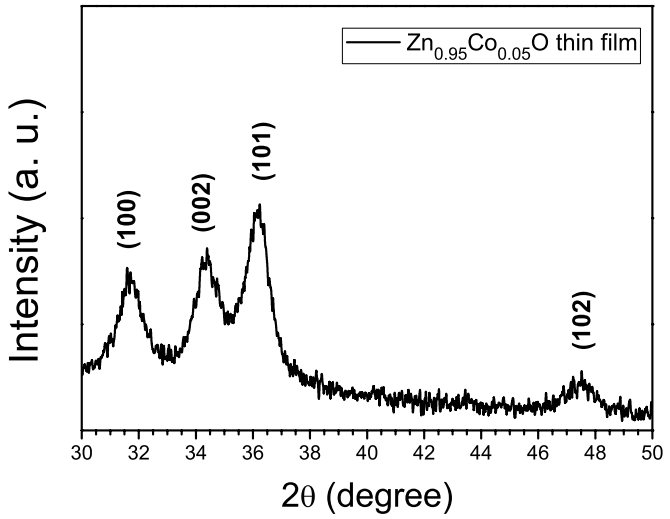

Fig. 1. The GI-XRD pattern of as-prepared $Zn_{0.95}Co_{0.05}O$ thin film shows the wurtzite structure without secondary phases.

which could contribute to the enhancement of sensing processes and properties [25]. Among the chemical/physical techniques to obtain oxides-based thin films for industrial purposes, the spray-pyrolysis presents advantages as versatility, low-cost route and large area production for the development of such devices [37].

This manuscript addresses the ozone gas-sensing performance of the nominal $Zn_{0.95}Co_{0.05}O$ thin films deposited via spray-pyrolysis technique for application as ozone gas sensors. The microstructural and surface properties were investigated by glancing incidence X-ray diffraction (GI-XRD), atomic force microscopy (AFM), field emission scanning electron microscopy (FE-SEM), X-ray photoelectron spectroscopy (XPS) measurements. DC electrical measurements indicated a good sensitive for different O_3 levels (20 to 1040 ppb). The film obtained by this route presented a good reproducibility, long-term stability, and high selectivity towards O_3 gas. These findings demonstrate its potential for practical applications in environmental monitoring.

2. Experimental section

2.1. Thin film deposition

The nominal $Zn_{0.95}Co_{0.05}O$ thin film was deposited via spray pyrolysis technique on SiO_2/Si substrate containing Pt interdigitated electrodes (120 nm thick). The precursor solution (0.004 M) was prepared by proportional mixing of aqueous solutions (distilled water) containing zinc acetate dihydrate ($Zn(CH_3OO)_2{\cdot}2H_2O$, Synth) and cobalt acetate tetrahydrate ($Co(CH_3OO)_2{\cdot}4H_2O$, Synth). The deposition process was performed in a temperature range between 220 and 300 °C with a solution flow rate of 0.25 ml min^{-1} and using compressed air as the gas carrier (0.1 MPa). Further details regarding the thin film preparation may be found in reference [28].

2.2. Characterization techniques

The phase composition of $Zn_{0.95}Co_{0.05}O$ thin film was examined by glancing incidence X-ray diffraction (GI-XRD) using a *Rigaku Rotaflex* diffractometer RU-200B model with a Cu-Kα radiation source (λ = 1.5406 Å). Surface morphology analysis was carried out by *Zeiss*

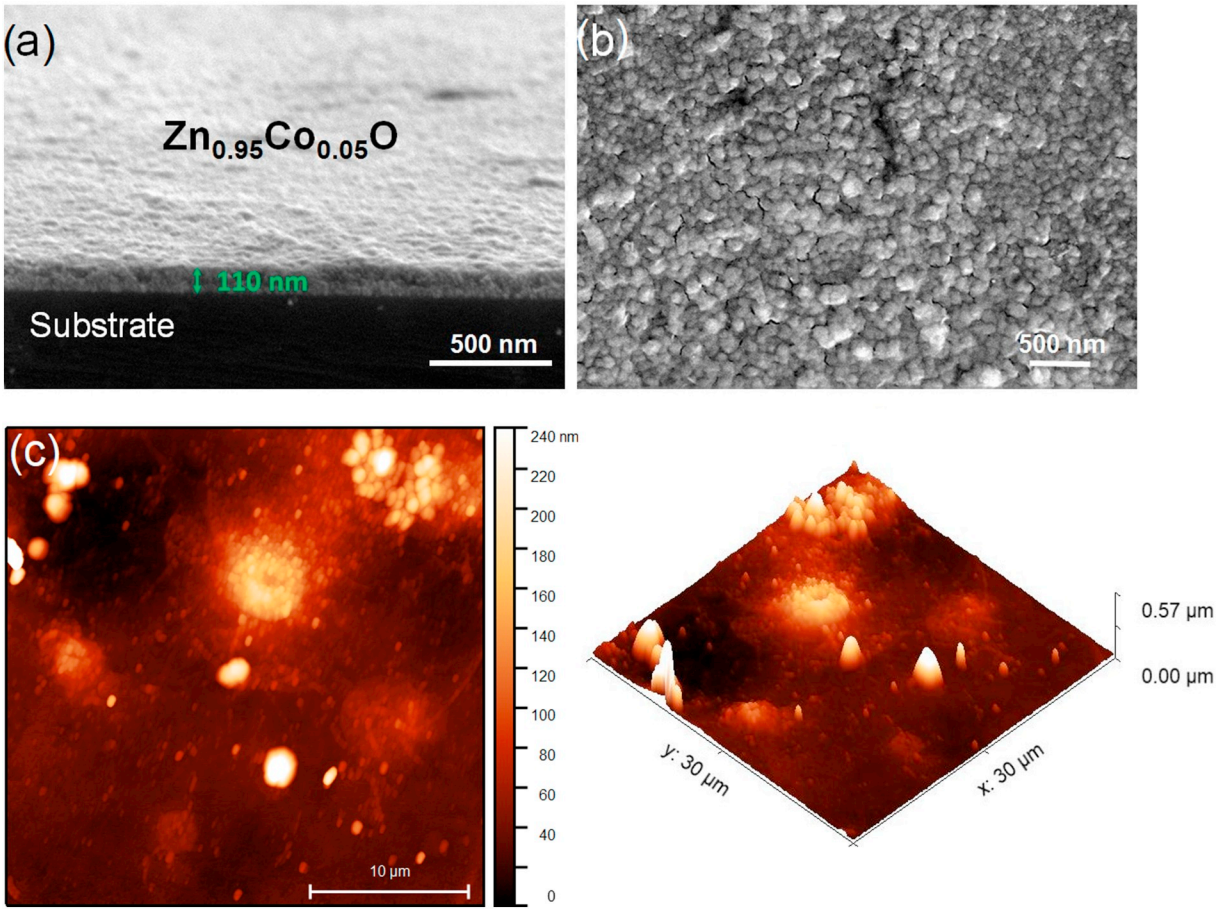

Fig. 2. Images of $Zn_{0.95}Co_{0.05}O$ thin film. (a) SEM cross-sectional and (b) surface views of the sample. (c) AFM in the 2D and 3D views.

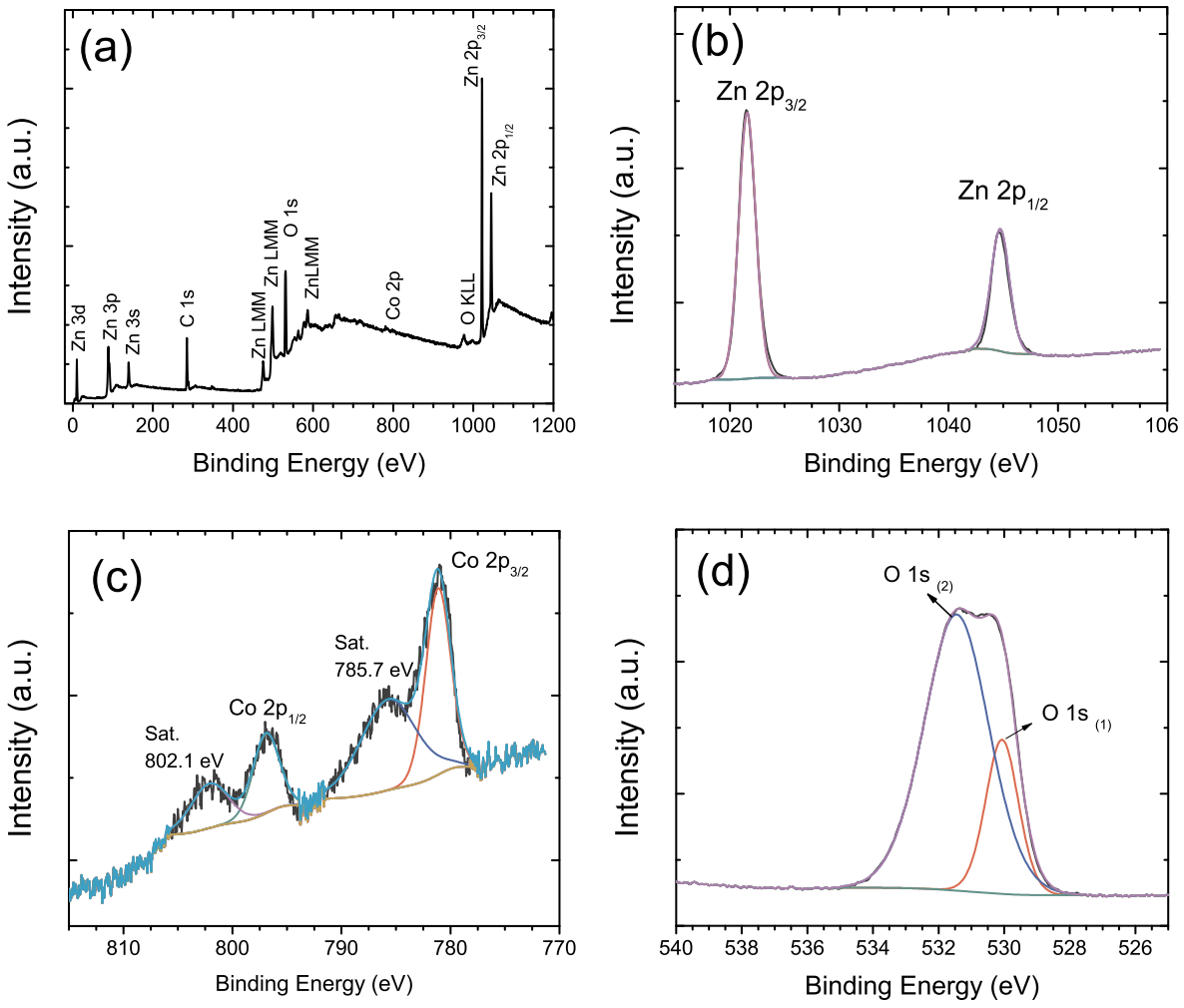

Fig. 3. XPS spectra of as-prepared $Zn_{0.95}Co_{0.05}O$ sample. (a) Survey scan, (b) Zn 2p, (c) Co 2p, and (d) O 1s.

SUPRA35 Scanning Electron Microscope operated at 5 kV and an atomic force microscope (Park Systems, model NX-10) in tapping mode. X-ray photoelectron spectroscopy (XPS) measurements were performed on a Thermo Scientific K-Alpha spectrometer using monochromatic Al-Kα (1486.6 eV) radiation. The peak decomposition was carried out using a 70% Gaussian and 30% Lorentzian line shape with a Shirley nonlinear sigmoid-type baseline. The binding energies were corrected for charging effects by assigning a value of 284.8 eV to the adventitious C 1s line. The XPS data were analyzed using CasaXPS software (Casa Software Ltd., U.K.).

2.3. Gas-sensing measurements

The as-prepared nominal $Zn_{0.95}Co_{0.05}O$ thin film was inserted into a chamber which allows both controls of the temperature (up to 350 °C) and different ozone concentrations, i.e., from 20 to 1040 ppb. Further details regarding the gas-sensing workbench may be found in reference [38]. Before each measurement, the sample was exposed to synthetic dry air (500 SCCM) during approximately 60 min to remove the impurities in the gas-sensing system. The O_3-containing dry air (constant flux of 500 SCCM) was blown directly onto the sample surface. To investigate the selectivity parameter, oxidizing and reducing gases were employed in a various concentration range. Before the experiments, the gas levels were calibrated using a toxic gas detector (ATI, model F12). For each cycle, the sample was exposed during 60 s towards to the target gas. The electrical resistance was measured by an electrometer (Keithley, model 6514) applying a *dc* voltage of 1 V. The sensor response (S) was defined as the relative electrical resistance variation, $S = (R_{O3} - R_{air}) / R_{air} = \Delta R / R$, where R_{O3} and R_{air} are the sensor electrical resistance upon exposure to O_3 gas and dry air. The sensor response time was defined as the time required electrical resistance to reach 90% of the final value when exposed to the target gas. The recovery time was defined as the time required electrical resistance to recover 90% of the initial value after the gas flow is switched off.

3. Results and discussions

The GI-XRD pattern of $Zn_{0.95}Co_{0.05}O$ thin film is shown in Fig. 1. The reflections presented in the XRD pattern were indexed as a hexagonal wurtzite structure of ZnO phase with a $P6_3mc$ space group (JCPDS file 36-1451). Furthermore, we did not observe any peak related to spurious phases, within the detection limit of equipment.

Fig. 2(a) showed a homogeneous film exhibiting a thickness of approximately 110 nm and good adhesion to the substrate. In addition, the Fig. 2(b) e 2(c) reveals that the sample presents a texturized surface with a root-mean-square roughness (R_{rms}) value of approximately 35 nm. The surface texturization is attributed to grains formation with an average size of 120 nm.

The XPS technique was performed to analyze the electronic structure at the surface of $Zn_{0.95}Co_{0.05}O$ film. Fig. 3(a) displays the XPS survey spectrum of the as-prepared $Zn_{0.95}Co_{0.05}O$ film, which revealed the existence of only Zn, Co, O, and C. It should be mentioned the difficulty to detect the Co 2p peak due to low Co content in the sample. The atomic concentration of Zn, Co and O were determined from the

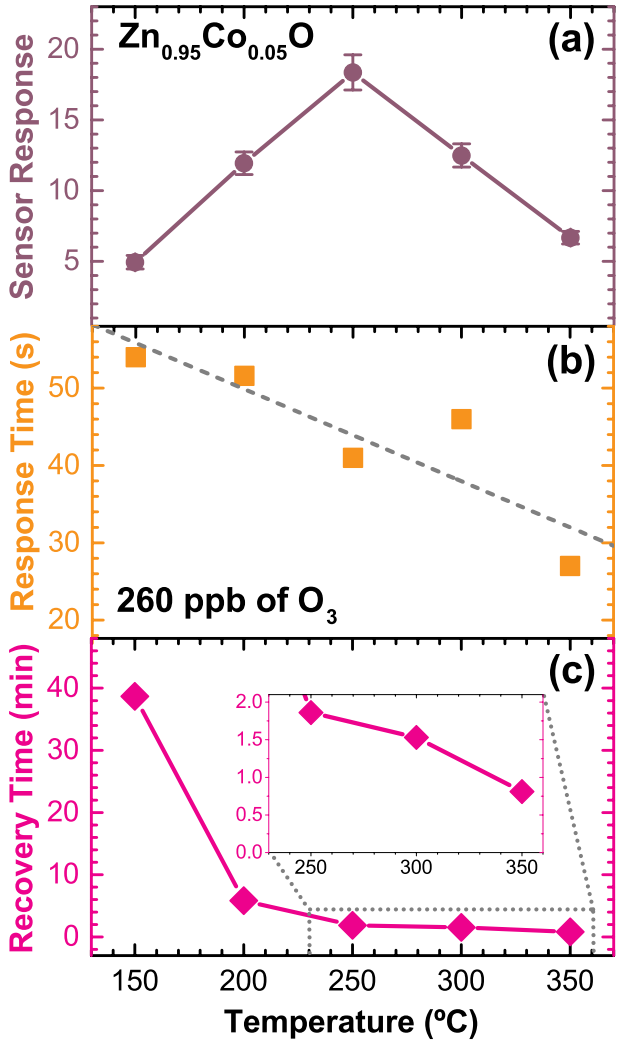

Fig. 4. (a) Gas sensor response (b) Response time (c) Recovery time (the inset shows a zoom at low recovery times) of $Zn_{0.95}Co_{0.05}O$ thin film exposed to 260 ppb O_3 as a function of the working temperature.

survey spectrum as 25.0, 0.8% and 74.2%, respectively. To estimate the Zn/O ratio, only the oxygen species-related from Zn—O bonds are considered from the analysis of the O 1s high-resolution spectrum. From O 1s high-resolution spectrum, only 21.8% corresponds to oxygen species related to ZnO phase, whereas 78.2% corresponds to adsorbed molecular oxygen from the atmosphere on the oxide thin film. If we consider only the oxygen species related to ZnO phase (530.1 eV), the Zn/O ratio is equal to 1.15, close to the value of 1 that should be obtained. This difference could be due to the O—Co contribution at 530.1 eV for O 1s peak that was not considered in the calculation.

In the high-resolution Zn 2p XPS spectrum shown in Fig. 3(b), the Zn $2p_{3/2}$ and Zn $2p_{1/2}$ peaks are located at 1022.3 eV and 1045.4 eV, respectively, which confirms the presence of only Zn^{2+} ions [39]. The high-resolution Co 2p XPS spectrum reveals the Co element existence in the sample, as seen in Fig. 3(c). The spectrum exhibits two major peaks with binding energy values of 781.1 eV and 796.9 eV, corresponding to Co $2p_{3/2}$ and Co $2p_{1/2}$ doublet core level peaks. These binding energy values are comparable to that reported for CoO indicating the presence of Co^{2+} species [39,40]. Additionally, the formation of divalent Co ions is supported by the presence of shakeup satellite located at a binding energy value of 785.7 eV and 802.1 eV [39].

Fig. 3(d) shows the O 1s spectrum of the $Zn_{0.95}Co_{0.05}O$ sample, deconvoluted into two components, labeled as O $1s_{(1)}$ (530.1 eV) and O $1s_{(2)}$ (531.2 eV). The O $1s_{(1)}$ peak corresponds to the oxygen species (O^{2-}) located in lattice bound to the metal cations (Zn^{2+} or substitutional Co^{2+}), while the O $1s_{(2)}$ peak reveals the presence of hydroxyl groups adsorbed on the sample surface. It should note here that the peak at approximately 531.2 eV was also attributed to the existence of oxygen vacancies or defects at the sample surface or oxygen deficient regions within the ZnO lattice.

Electrical measurements were used to investigate the gas-sensing properties of $Zn_{0.95}Co_{0.05}O$ thin film. It is known that the operating temperature is an important parameter to be quantified as long as it governs the adsorption/desorption processes of specimens in the surface and the electrical conductivity [8].

In this way, to determine the optimal working temperature, the film was exposed to 260 ppb of O_3 at different temperatures. The reversible cycles of exposure presented in Fig. S1 (Support information) show that the sample electrical resistance increases after O_3 exposition, typical behavior for n-type semiconductors in oxidant atmospheres [41]. For an exposition to 260 ppb, the sensor response O_3 as a function of the working temperature is presented in Fig. 4(a). It should be noted that the highest response of film is found at approximately 250 °C. This temperature is within the range reported to sensing materials commonly used as conductometric heated ozone sensors (200–400 °C). Some of these ozone sensor materials can also be operated at room temperature (RT) with UV radiation. Overall, conductometric ozone sensors operate in temperatures from RT to 400 °C and detect gas concentration levels of few to thousand ppb [42]. A summary of several materials used in ozone sensing fabricated by many chemical/physical

Table 1
Summary of results for ozone gas sensors based on several metal oxide semiconductors prepared by different methodologies.

Material	Preparation method	Operating temperature (°C)	Sensor response	Response/Recovery time (s)	Minimum O_3 level detected (ppb)	Gases tested	Reference
SnO_2	Spray pyrolysis	200	10^3 [d]	n/a	1000	O_3	[10]
SnO_2	Successive Ionic Layer Deposition (SILD)	200	~10^5 [d]	4/100	1000	O_3	[43]
SnO_2 (triton)	Spin coating	RT	3 [d]	15/720	500	O_3	[44]
SnO_2:2%Co	Spray pyrolysis	270	10^4 [d]	n/a	1000	O_3, H_2, LPG, CO	[45]
WO_3	RF-magnetron sputtering	250	16 [a]	1/ < 60	30	O_3	[46]
$ZnCo_2O_4$	Co-precipitation	200	0.23 [b]	8/10	80	O_3, NO_2, CO,NH_3	[47]
$SrTi_{0.85}Fe_{0.15}O_3$	Electron beam deposition	260	~3 [c]	26/72	100	O_3, NO_2, CO,NH_3	[38]
In_2O_3	Spray pyrolysis	250	10^3 [d]	~10/180	1000	O_3	[11]
In_2O_3	Sol-gel	100	20 [e]	n/a	200	O_3, NO_2	[48]
In_2O_3	MOCVD	RT (UV)	~4 [d]	n/a	10	O_3	[49]
ZnO-SnO_2	Hydrothermal	RT (UV)	8 [d]	n/a	20	O_3, NO_2, CO, NH_3	[50]
Pt/TiO_2- SnO_2	Dip coating	RT (UV)	~250 [d]	1000/	500	O_3	[51]
ZnO	Hydrothermal	250	~3 [d]	~9/300	60	O_3	[12]
ZnO	Chemical vapor deposition	200	~10^2 [e]	n/a	280	O_3, NO_2, Acetone, Ethanol	[13]

(*continued on next page*)

Table 1 (*continued*)

Material	Preparation method	Operating temperature (°C)	Sensor response	Response/Recovery time (s)	Minimum O_3 level detected (ppb)	Gases tested	Reference
$Zn_{0.95}Co_{0.05}O$	Polymeric precursors	200	~3 [e]	46/360	42	O_3, NO_2, CO	[39]
$Zn_{0.95}Co_{0.05}O$	Spray pyrolysis	250	0.4 [e]	46/62	20	O_3, NO_2, NH_3, CO	Present study

[a] $S = \frac{G_{air}}{G_{gas}}$.
[b] $S = \frac{R_{air} - R_{gas}}{R_{air}}$.
[c] $S = \frac{R_{air}}{R_{gas}}$.
[d] $S = \frac{R_{gas}}{R_{air}}$.
[e] $S = \frac{R_{gas} - R_{air}}{R_{air}}$.

techniques is displayed in Table 1, which contains functional parameters like response/recovery times, minimum ozone levels and specimens selectivity.

Fig. 4(b)–(c) depict the response and recovery times of $Zn_{0.95}Co_{0.05}O$ film exposed to 260 ppb of O_3. These data reflect the influence of adsorption/desorption mechanisms of O_3 on the sample surface. The resistance increase in O_3 content atmosphere can be linked to the capture of free electrons by the oxygen specimens adsorbed at the film surface [10]. At a first approximation, the response time decreases linearly with temperature ($-0.12\,°C^{-1}$) and the optimum operating temperature at 250 °C corresponds to around 40 s. The desorption of ionized specimens is less efficient and the recovery time increases significantly and exhibiting an exponential behavior with a recovery time of around 100 s at 250 °C.

The ozone sensing response of $Zn_{0.95}Co_{0.05}O$ film is displayed in Fig. 5(a) for different concentrations of O_3 (20 to 1040 ppb) at an operating temperature of 250 °C. The material showed a noticeable response to ozone as well as good reproducibility considering 3 exposition cycles. Considering the harmful limit for human health, considerable progress on the evaluation of chemiresistor based on $Zn_{1-x}Co_xO$ compound is achieved considering the increase from 50 to 100% for the electrical resistance when the O_3 level is 20 ppb and 89 ppb respectively. In addition, response and recovery times are in the order of 1 min. Fig. 5(b) shows the dependence of sensor response and ozone level detected by as-prepared $Zn_{0.95}Co_{0.05}O$ thin film. It can be seen that the predicted lower detection limit in a linear approximation is around 7 ppb of O_3 gas.

The selectivity is an essential parameter for the sensing element that specifies the ability of the sensor to discriminate the response of the different analytes. The response of as-prepared $Zn_{0.95}Co_{0.05}O$ film was then studied to different target gases (NO_2, NH_3, and CO). The sample was kept at 250 °C and then exposed to different concentrations of NO_2 (200 to 2000 ppb), NH_3 (5 to 500 ppm), and CO (5 to 500 ppm) gases. As depicted in Fig. 6(a)–(b), the sensor showed a response to NO_2 with good repeatability. It is important to note that after several exposure cycles to NO_2 gas the $Zn_{0.95}Co_{0.05}O$ film detected lowest gas concentration, demonstrating its total reversibility. Additionally, it was observed that the sensing material did not reach saturation towards both O_3 and NO_2 gases, even at the highest concentration obtained in our workbench. However, the response for NO_2 is quite lower as compared to O_3 gas. To reach a response of approximately 1, it would be necessary 200 ppb of NO_2 and an increase to 2000 ppb shows a response of approximately 4, effectively smaller as compared to the response around 60 observed when O_3 level is around 800 ppb.

Regarding the reducing gases, any sensitivity to different gas levels of CO is observed, while for NH_3 gas (Fig. 6(b)), it can be seen a low sensitivity and similar response independently of NH_3 levels. This behavior suggests that the sample reached the saturation level even for the lowest NH_3 level.

Fig. 7 presents the comparison of the sensor response (S) values of the $Zn_{0.95}Co_{0.05}O$ thin film at an operating temperature of 250 °C exposed to the different gases, i.e., 0.8 ppm of O_3, and 1.0 ppm of NO_2, NH_3, and CO. It can be observed that the sensor presented a high response to O_3 (49), less response to NO_2 (4.3), and NH_3 (0.1) and no response to CO gas. As can be seen, the sensor response to O_3 gas was approximately 10 and 500 times greater than to NO_2 and NH_3 respectively, indicating that the nanocrystalline $Zn_{0.95}Co_{0.05}O$ thin film obtained can be considered as a promising material for ozone gas sensors.

To evaluate the long-term stability, the as-prepared $Zn_{0.95}Co_{0.05}O$ film was kept at 250 °C and then exposed to 297 ppb of O_3 for 9 days, as

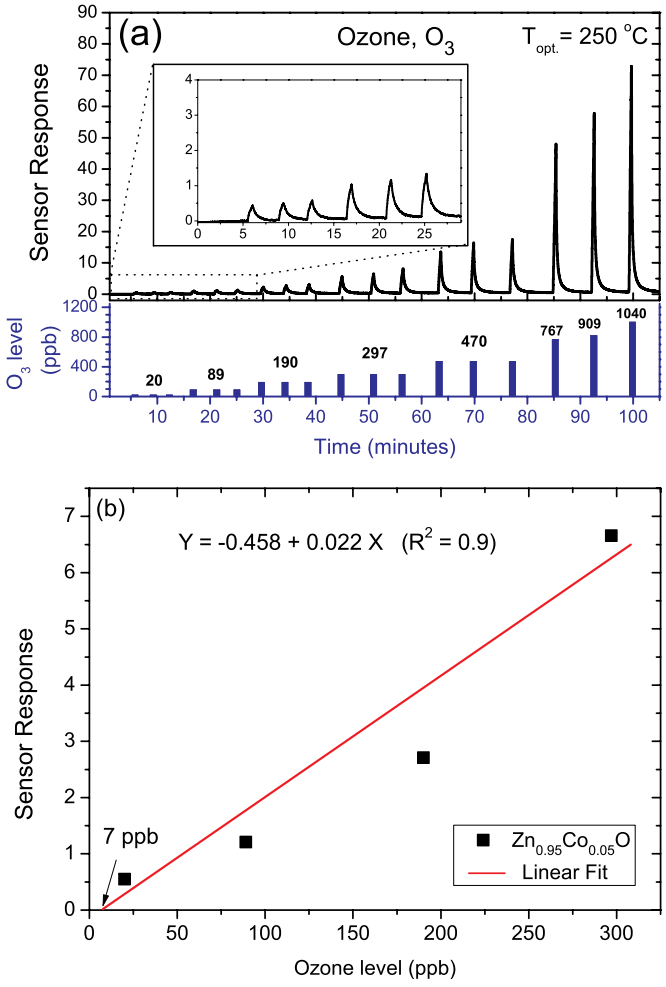

Fig. 5. (a) Ozone sensor response of $Zn_{0.95}Co_{0.05}O$ thin film at 250 °C exposed to different ozone levels (20 to 1040 ppb). The inset of panel (a) shows a detailed region of sensor response towards 20 and 89 ppb of O_3 gas. (b) A linear relationship between sensor response and ozone level was used to estimate the predicted minimum level detectable (20 to 297 ppb).

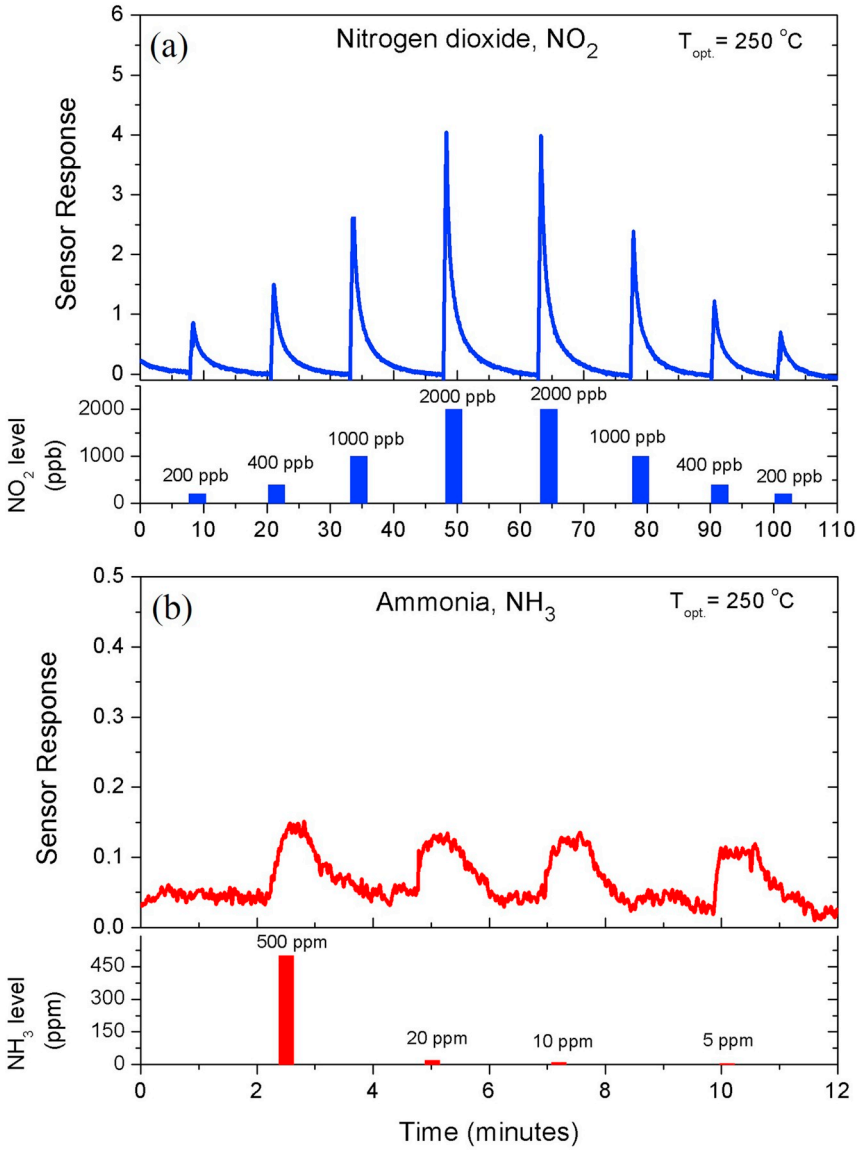

Fig. 6. Sensor response of $Zn_{0.95}Co_{0.05}O$ film at 250 °C exposed to different levels of (a) NO_2, and (b) NH_3 gas.

showed in Fig. 8. It can be seen that the response varied slightly in the period evaluated. Such results demonstrate the good stability of the nanostructured $Zn_{0.95}Co_{0.05}O$ thin film obtained via spray-pyrolysis technique.

3.1. Final remarks

A small amount of Co in the ZnO (nominally 5%) provided ozone sensor activity with good selectivity concerning the oxidant and reducing gases employed in this investigation. The presented results evidence the potential of nanostructured $Zn_{1-x}Co_xO$ thin film obtained via spray-pyrolysis, however, further investigations should be performed. In fact, the influence of humidity levels can affect the sensor response as the water molecules could compete with the ozone molecules by the same active sites. Future approaches include the optimization and calculations about the stability of ZnCoO surface and the role of Co presence to develop a realistic model for the analyte interaction. In-situ and *operando* investigations employing impedance spectroscopy can also give an insight into the gas sensing mechanisms of the as-synthesized $Zn_{1-x}Co_xO$ thin films.

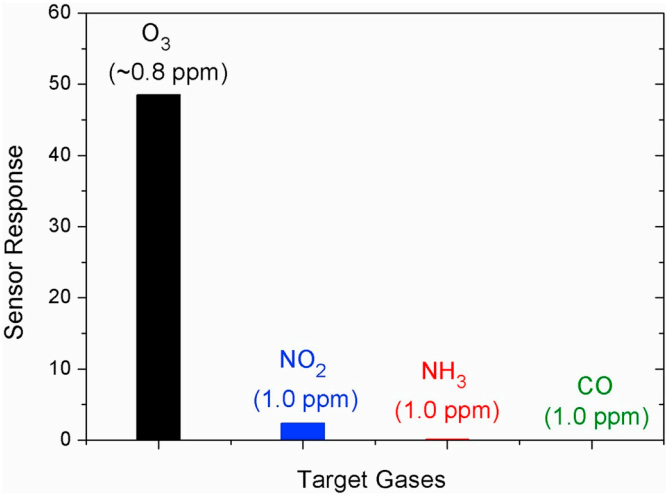

Fig. 7. Comparison of the sensor responses of the $Zn_{0.95}Co_{0.05}O$ thin film exposed towards different gases at an operating temperature of 250 °C.

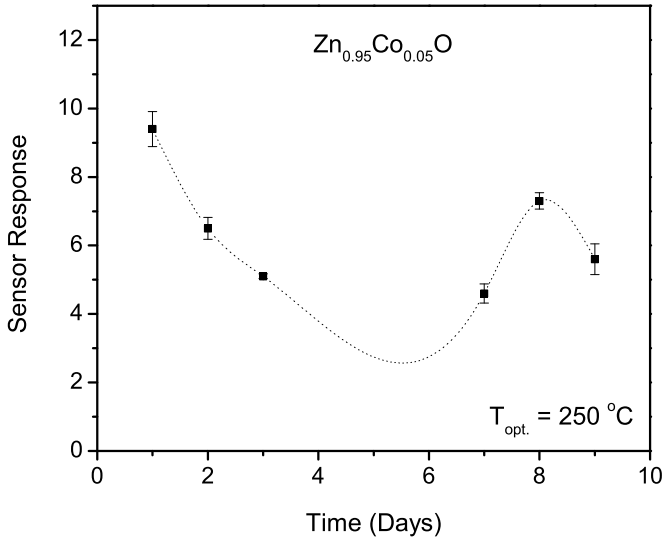

Fig. 8. Ozone sensor response of as-prepared $Zn_{0.95}Co_{0.05}O$ thin film kept at 250 °C and exposed 297 ppb of O_3 gas for 9 days.

4. Conclusions

Spray-pyrolysis was employed to produce a nominal $Zn_{0.95}Co_{0.05}O$ thin film as a gas sensor device. This method of synthesis discards the needs of vacuum or high temperatures and provides an effective approach to produce thin films in a two-steps process (preparation of precursor solution and pulverization/pyrolysis). The film surface has a homogeneous and rough character with nanosized grains. The XPS analyses revealed the incorporation of Co^{2+} into the ZnO lattice. With respect to sensing performance, the $Zn_{0.95}Co_{0.05}O$ thin film presents suitable repeatability, good range of detection (20 to 1040 ppb) to ozone gas, and low sensitivity to reducing gases (NH_3 and CO). Therefore, our results indicate a high selective material for thin film based ozone gas sensors obtained by a suitable and large-scale production method.

Acknowledgments

We are grateful to Mr. Rorivaldo Camargo for operating FE-SEM microscope. This work was supported by the following Brazilian research financing institutions: FAPESP (Proc. No. 2013/07296-2, 2016/10973-4 and 2017/12437-5), CNPq, and CAPES. The research was partially performed at the Brazilian Nanotechnology National Laboratory (LNNano) (Projects LMF-18580; XPS-22923 and AFM-23724) in Campinas, SP, Brazil.

Appendix A. Supplementary data

Supplementary data to this article can be found online at https://doi.org/10.1016/j.apsusc.2019.01.197.

References

[1] R. Dhahri, S.G. Leonardi, M. Hjiri, L. El Mir, A. Bonavita, N. Donato, D. Iannazzo, G. Neri, Enhanced performance of novel calcium/aluminum co-doped zinc oxide for CO2 sensors, Sensors Actuators B Chem. 239 (2017) 36–44, https://doi.org/10.1016/J.SNB.2016.07.155.

[2] J.C. Liu, R.D. Peng, Health effect of mixtures of ozone, nitrogen dioxide, and fine particulates in 85 US counties, Air Qual. Atmos. Health 11 (2018) 311–324, https://doi.org/10.1007/s11869-017-0544-2.

[3] L. Guo, Y.-W. Hao, P.-L. Li, J.-F. Song, R.-Z. Yang, X.-Y. Fu, S.-Y. Xie, J. Zhao, Y.-L. Zhang, Improved NO 2 gas sensing properties of graphene oxide reduced by two-beam-laser interference, Sci. Rep. 81 (8) (2018) 4918, https://doi.org/10.1038/s41598-018-23091-1.

[4] H.F. Hemond, E.J. Fechner, H.F. Hemond, E.J. Fechner, The atmosphere, Chem. Fate Transp. Environ, Elsevier, 2015, pp. 311–454, , https://doi.org/10.1016/B978-0-12-398256-8.00004-9.

[5] P.S. Monks, A.T. Archibald, A. Colette, O. Cooper, M. Coyle, R. Derwent, D. Fowler, C. Granier, Tropospheric ozone and its precursors from the urban to the global scale from air quality to short-lived climate forcer, Atmos. Chem. Phys. 15 (2015) 8889–8973, https://doi.org/10.5194/acp-15-8889-2015.

[6] CETESB, Qualidade do ar no Estado de São Paulo 2016, http://cetesb.sp.gov.br/ar/wp-content/uploads/sites/28/2013/12/relatorio-ar-2016.pdf, (2017).

[7] D. Sauter, U. Weimar, G. Noetzel, J. Mitrovics, W. Göpel, Development of modular ozone sensor system for application in practical use, Sensors Actuators B Chem. 69 (2000) 1–9, https://doi.org/10.1016/S0925-4005(00)00295-1.

[8] G. Korotcenkov, V. Brinzari, B.K. Cho, In_2O_3- and SnO_2-based ozone sensors: design and characterization, Crit. Rev. Solid State Mater. Sci. 43 (2018) 83–132, https://doi.org/10.1080/10408436.2017.1287661.

[9] X. Zhou, S. Lee, Z. Xu, J. Yoon, Recent progress on the development of chemo-sensors for gases, Chem. Rev. 115 (2015) 7944–8000, https://doi.org/10.1021/cr500567r.

[10] G. Korotcenkov, I. Blinov, M. Ivanov, J.R. Stetter, Ozone sensors on the base of SnO2 films deposited by spray pyrolysis, Sensors Actuators B Chem. 120 (2007) 679–686, https://doi.org/10.1016/J.SNB.2006.03.029.

[11] G. Korotcenkov, A. Cerneavschi, V. Brinzari, A. Vasiliev, M. Ivanov, A. Cornet, J. Morante, A. Cabot, J. Arbiol, In2O3 films deposited by spray pyrolysis as a material for ozone gas sensors, Sensors Actuators B Chem. 99 (2004) 297–303, https://doi.org/10.1016/J.SNB.2003.01.001.

[12] A.C. Catto, L.F. da Silva, C. Ribeiro, S. Bernardini, K. Aguir, E. Longo, V.R. Mastelaro, An easy method of preparing ozone gas sensors based on ZnO nanorods, RSC Adv. 5 (2015) 19528–19533, https://doi.org/10.1039/C5RA00581G.

[13] D. Barreca, D. Bekermann, E. Comini, A. Devi, R.A. Fischer, A. Gasparotto, C. Maccato, C. Sada, G. Sberveglieri, E. Tondello, Urchin-like ZnO nanorod arrays for gas sensing applications, CrystEngComm 12 (2010) 3419, https://doi.org/10.1039/c0ce00139b.

[14] J. Guérin, M. Bendahan, K. Aguir, A dynamic response model for the WO3-based ozone sensors, Sensors Actuators B Chem. 128 (2008) 462–467, https://doi.org/10.1016/J.SNB.2007.07.010.

[15] A. Tsukazaki, M. Kubota, A. Ohtomo, T. Onuma, K. Ohtani, H. Ohno, S.F. Chichibu, M. Kawasaki, Blue light-emitting diode based on ZnO, Jpn. J. Appl. Phys. 44 (2005) L643–L645, https://doi.org/10.1143/JJAP.44.L643.

[16] S.J. Chang, Y.K. Su, Y.P. Shei, High quality ZnO thin films on InP substrates prepared by radio frequency magnetron sputtering. II. Surface acoustic wave device fabrication, J. Vac. Sci. Technol. A 13 (1995) 385–388, https://doi.org/10.1116/1.579368.

[17] T. Söderström, D. Dominé, A. Feltrin, M. Despeisse, F. Meillaud, G. Bugnon, M. Boccard, P. Cuony, F.-J. Haug, S. Faÿ, S. Nicolay, C. Ballif, ZnO transparent conductive oxide for thin film silicon solar cells, in: F.H. Teherani, D.C. Look, C.W. Litton, D.J. Rogers (Eds.), International Society for Optics and Photonics, 2010, p. 76030B, , https://doi.org/10.1117/12.843511.

[18] H.S. Al-Salman, M.J. Abdullah, Hydrogen gas sensing based on ZnO nanostructure prepared by RF-sputtering on quartz and PET substrates, Sensors Actuators B Chem. 181 (2013) 259–266, https://doi.org/10.1016/J.SNB.2013.01.065.

[19] M.J.S. Spencer, I. Yarovsky, ZnO nanostructures for gas sensing: interaction of NO_2, NO, O, and N with the ZnO$(10\bar{1}0)$ surface, J. Phys. Chem. C 114 (2010) 10881–10893, https://doi.org/10.1021/jp1016938.

[20] Z.S. Hosseini, A.I. zad, A. Mortezaali, Room temperature H2S gas sensor based on rather aligned ZnO nanorods with flower-like structures, Sensors Actuators B Chem. 207 ((2015) 865–871, https://doi.org/10.1016/J.SNB.2014.10.085.

[21] Q. Wan, Q.H. Li, Y.J. Chen, T.H. Wang, X.L. He, J.P. Li, C.L. Lin, Fabrication and ethanol sensing characteristics of ZnO nanowire gas sensors, Appl. Phys. Lett. 84 (2004) 3654–3656, https://doi.org/10.1063/1.1738932.

[22] J. Xu, Y. Shun, Q. Pan, J. Qin, Sensing characteristics of double layer film of ZnO, Sensors Actuators B Chem. 66 (2000) 161–163, https://doi.org/10.1016/S0925-4005(00)00327-0.

[23] D. Gupta, D. Dutta, M. Kumar, P.B. Barman, T. Som, S.K. Hazra, Temperature dependent dual hydrogen sensor response of Pd nanoparticle decorated Al doped ZnO surfaces, J. Appl. Phys. 118 (2015) 164501, , https://doi.org/10.1063/1.4934521.

[24] T. Çorlu, I. Karaduman, S. Galioglu, B. Akata, M.A. Yıldırım, A. Ateş, S. Acar, Low level NO gas sensing properties of Cu doped ZnO thin films prepared by SILAR method, Mater. Lett. 212 (2018) 292–295, https://doi.org/10.1016/J.MATLET.2017.10.121.

[25] D. Sett, D. Basak, Highly enhanced H2 gas sensing characteristics of Co:ZnO nanorods and its mechanism, Sensors Actuators B Chem. 243 (2017) 475–483, https://doi.org/10.1016/j.snb.2016.11.163.

[26] V.S. Bhati, S. Ranwa, M. Fanetti, M. Valant, M. Kumar, Efficient hydrogen sensor based on Ni-doped ZnO nanostructures by RF sputtering, Sensors Actuators B Chem. 255 (2018) 588–597, https://doi.org/10.1016/J.SNB.2017.08.106.

[27] R. Ciprian, C. Baratto, A. Giglia, K. Koshmak, G. Vinai, M. Donarelli, M. Ferroni, M. Campanini, E. Comini, A. Ponzoni, G. Sberveglieri, Magnetic gas sensing exploiting the magneto-optical Kerr effect on ZnO nanorods/Co layer system, RSC Adv. 6 (2016) 42517–42521, https://doi.org/10.1039/C6RA00522E.

[28] Y.J. Onofre, S. de Castro, A.D. Rodrigues, M.P.F. de Godoy, Influence of Co-doping on optical properties and traps localization of ZnO films obtained by spray pyrolysis, J. Anal. Appl. Pyrolysis 128 (2017) 131–135, https://doi.org/10.1016/J.JAAP.2017.10.017.

[29] A. Albert manoharan, R. Chandramohan, K.D. Arun Kumar, S. Valanarasu, V. Ganesh, M. Shkir, H. Algarni, S. AlFaify, Transition metal (Mn) and rare earth (Nd) di-doped novel ZnO nanoparticles: a facile sol–gel synthesis and characterization, J. Mater. Sci. Mater. Electron. (2018) 1–10, https://doi.org/10.1007/

s10854-018-9430-4.
[30] N.L. Tarwal, K.V. Gurav, T. Prem Kumar, Y.K. Jeong, H.S. Shim, I.Y. Kim, J.H. Kim, J.H. Jang, P.S. Patil, Structure, X-ray photoelectron spectroscopy and photoluminescence investigations of the spray deposited cobalt doped ZnO thin films, J. Anal. Appl. Pyrolysis 106 (2014) 26–32, https://doi.org/10.1016/j.jaap.2013.12.005.
[31] S.-L. Ou, H.-R. Liu, S.-Y. Wang, D.-S. Wuu, Co-doped ZnO dilute magnetic semiconductor thin films by pulsed laser deposition: excellent transmittance, low resistivity and high mobility, J. Alloys Compd. 663 (2016) 107–115, https://doi.org/10.1016/j.jallcom.2015.12.101.
[32] E. Bacaksiz, S. Aksu, B.M. Basol, M. Altunbaş, M. Parlak, E. Yanmaz, Structural, optical and magnetic properties of Zn1 − xCoxO thin films prepared by spray pyrolysis, Thin Solid Films 516 (2008) 7899–7902, https://doi.org/10.1016/j.tsf.2008.03.042.
[33] V. Gandhi, R. Ganesan, H.H. Abdulrahman Syedahamed, M. Thaiyan, Effect of cobalt doping on structural, optical, and magnetic properties of ZnO nanoparticles synthesized by coprecipitation method, J. Phys. Chem. C 118 (2014) 9715–9725, https://doi.org/10.1021/jp411848t.
[34] G.K. Mani, J.B.B. Rayappan, A highly selective and wide range ammonia sensor—nanostructured ZnO:Co thin film, Mater. Sci. Eng. B 191 (2015) 41–50, https://doi.org/10.1016/J.MSEB.2014.10.007.
[35] V.V. Ganbavle, S.K. Patil, S.I. Inamdar, S.S. Shinde, K.Y. Rajpure, Effect of Co doping on structural, morphological and LPG sensing properties of nanocrystalline ZnO thin films, Sensors Actuators A Phys. 216 (2014) 328–334, https://doi.org/10.1016/J.SNA.2014.06.009.
[36] A.J. Kulandaisamy, C. Karthek, P. Shankar, G.K. Mani, J.B.B. Rayappan, Tuning selectivity through cobalt doping in spray pyrolysis deposited ZnO thin films, Ceram. Int. 42 (2016) 1408–1415, https://doi.org/10.1016/j.ceramint.2015.09.084.
[37] Y.J. Onofre, S. de Castro, M.P.F. de Godoy, Effect of traps localization in ZnO thin films by photoluminescence spectroscopy, Mater. Lett. 188 (2017) 37–40, https://doi.org/10.1016/j.matlet.2016.10.081.
[38] L.F. da Silva, V.R. Mastelaro, A.C. Catto, C.A. Escanhoela, S. Bernardini, S.C. Zílio, E. Longo, K. Aguir, Ozone and nitrogen dioxide gas sensor based on a nanostructured SrTi0.85Fe0.15O3 thin film, J. Alloys Compd. 638 (2015) 374–379, https://doi.org/10.1016/J.JALLCOM.2015.03.089.
[39] A.C. Catto, L.F. da Silva, M.I.B. Bernardi, S. Bernardini, K. Aguir, E. Longo, V.R. Mastelaro, Local structure and surface properties of CoxZn1-xO thin films for ozone gas sensing, ACS Appl. Mater. Interfaces 8 (2016) 26066–26072, https://doi.org/10.1021/acsami.6b08589.
[40] D. Bekermann, A. Gasparotto, D. Barreca, A. Devi, R.A. Fischer, p-Co_3O_4/n-ZnO, obtained by PECVD, analyzed by X-ray photoelectron spectroscopy, Surf. Sci. Spectra 18 (2011) 36–45, https://doi.org/10.1116/11.20111003.
[41] G.F. Fine, L.M. Cavanagh, A. Afonja, R. Binions, Metal oxide semi-conductor gas sensors in environmental monitoring, Sensors 10 (2010) 5469–5502, https://doi.org/10.3390/s100605469.
[42] G. Korotcenkov, V. Brinzari, B.K. Cho, In_2O_3- and SnO_2-based thin film ozone sensors: fundamentals, J. Sens. 2016 (2016) 1–31, https://doi.org/10.1155/2016/3816094.
[43] G. Korotcenkov, B.K. Cho, L. Gulina, V. Tolstoy, Ozone sensors based on SnO2 films modified by SnO2–Au nanocomposites synthesized by the SILD method, Sensors Actuators B Chem. 138 (2009) 512–517, https://doi.org/10.1016/J.SNB.2009.01.058.
[44] M. Belaqziz, M. Amjoud, A. Gaddari, B. Rhouta, D. Mezzane, Enhanced room temperature ozone response of SnO2 thin film sensor, Superlattice. Microst. 71 (2014) 185–189, https://doi.org/10.1016/J.SPMI.2014.03.040.
[45] G. Korotcenkov, I. Boris, V. Brinzari, S.H. Han, B.K. Cho, The role of doping effect on the response of SnO2-based thin film gas sensors: analysis based on the results obtained for Co-doped SnO2 films deposited by spray pyrolysis, Sensors Actuators B Chem. 182 (2013) 112–124, https://doi.org/10.1016/J.SNB.2013.02.103.
[46] M. Bendahan, R. Boulmani, J. Seguin, K. Aguir, Characterization of ozone sensors based on WO3 reactively sputtered films: influence of O2 concentration in the sputtering gas, and working temperature, Sensors Actuators B Chem. 100 (2004) 320–324, https://doi.org/10.1016/J.SNB.2004.01.023.
[47] N. Joshi, L.F. da Silva, H.S. Jadhav, F.M. Shimizu, P.H. Suman, J.-C. M'Peko, M.O. Orlandi, J.G. Seo, V.R. Mastelaro, O.N. Oliveira, Yolk-shelled ZnCo2O4 microspheres: surface properties and gas sensing application, Sensors Actuators B Chem. 257 (2018) 906–915, https://doi.org/10.1016/J.SNB.2017.11.041.
[48] M. Ivanovskaya, A. Gurlo, P. Bogdanov, Mechanism of O3 and NO2 detection and selectivity of In2O3 sensors, Sensors Actuators B Chem. 77 (2001) 264–267, https://doi.org/10.1016/S0925-4005(01)00708-0.
[49] C.Y. Wang, S. Bagchi, M. Bitterling, R.W. Becker, K. Köhler, V. Cimalla, O. Ambacher, C. Chaumette, Photon stimulated ozone sensor based on indium oxide nanoparticles II: ozone monitoring in humidity and water environments, Sensors Actuators B Chem. 164 (2012) 37–42, https://doi.org/10.1016/J.SNB.2012.01.058.
[50] L.F. da Silva, J.-C. M'Peko, A.C. Catto, S. Bernardini, V.R. Mastelaro, K. Aguir, C. Ribeiro, E. Longo, UV-enhanced ozone gas sensing response of ZnO-SnO2 heterojunctions at room temperature, Sensors Actuators B Chem. 240 (2017) 573–579, https://doi.org/10.1016/J.SNB.2016.08.158.
[51] R.-J. Wu, C.-Y. Chen, M.-H. Chen, Y.-L. Sun, Photoreduction measurement of ozone using Pt/TiO2–SnO2 material at room temperature, Sensors Actuators B Chem. 123 (2007) 1077–1082, https://doi.org/10.1016/J.SNB.2006.11.013.